CHAPTER V

EFFECTS OF THE CRUDE EXTRACT FROM *MUCUNA MACROCARPA* ON GONADAL STEROIDOGENESIS IN TILAPIA

INTRODUCTION

Reproductive effects of the extract from *Mucuna* species are well documented. The black Kwao Krua, *Mucuna macrocarpa* Wall. (synonym: *Mucuna collettii* Lace) has been used in traditional Thai remedy for treatment of male sexual dysfunction. The study on chemical constituents of this plant extract revealed three important compounds including kaempferol, quercetin and hopeaphenol (Roengsumran et al., 2001). Quercetin is an active compound that has been reported to cause adverse reproductive effects on both sexes (Eckberg, 1983; Aravindakshan et al., 1985; Nass-Arden and Breitbart, 1990; Khanduja et al., 2001). Hopeaphenol is a tetramer of a well known phytoestrogen, resveratrol which shows variable degrees of estrogen receptor agonist (Gehm et al., 1997). The dietary treatment of resveratrol reduced body weight, disrupted estrous cycle and induced ovarian hypertrophy in normal adult female rats (Henry and Witt, 2002). Reproductive effect of *M. macrocarpa* studied in rat showed that the 1-month treatment at 10-100 mg/kg had no effect on sex hormone levels and reproductive organs of the adult males; whereas in the females, it altered plasma sex hormone levels without histopathological alteration in the ovarian tissues (Thansa, 2003). Based on the fact that *M. macrocarpa* contains several hormonally active chemicals and its reproductive effects are documented, yet the effect on gonadal

steroidogenesis is still limited. It is of interest to know whether the crude extract from this plant can affect gonadal steroidogenic functions in the fish model.

The effects on steroidogenesis can be assessed using histochemical biomarker. 3β-hydroxysteroid dehydrogenase (3β-HSD) is an enzyme in early steroidogenic pathway that catalyzes conversion of pregnenolone to progesterone (Johnson and Everitt, 2000). It has been used in many studies as a key biomarker of steroidogenesis in target tissues (Guraya, 1976). In bony fish, the possible sites of steroidogenesis in ovary are both granulosa and thecal cells of growing follicles, corpora atretica and corpora lutea (Guraya, 1976), while the steroidogenic sites in testis are Leydig cells (van den Hurk, 1973; van den Hurk, 1974; Schreibman et al., 1982). In addition to the histochemical technique, cytological ultrastructures have been used by many researchers to confirm the steroidogenic potential of the tissue as reviewed by Guraya (1976).

To elucidate the effect of plant extract on reproductive organ, we used subchronic toxicity bioassay to assess reproductive effects of *M. macrocarpa* crude extract on gonadal steroidogenesis of the Nile tilapia, *Oreochromis niloticus*. Changes in gonadal steroidogenesis after exposure to plant extract were determined in the mature tilapia using histochemical and ultrastructural biomarkers. The target cells for the examination of steroidogenesis were the Leydig cell in the tilapia testis, and the granulosa cell and the thecal cell of the ovarian follicle.

MATERIALS AND METHODS

Fish procurement and maintenance

O. niloticus brood stock (3 weeks post-hatching) was obtained from the Aquatic Animal Breeding Research Station at Pathumtani, Department of Fisheries, the Ministry of Agriculture and Cooperatives of Thailand. The fish were raised in 325-L glass aquarium with aerated water. They were maintained on a 14 h light/10 h dark photoperiod at 27-29 °C and fed with commercial fish food (CP Company) twice daily. Water pH ranged between 6.6 and 7.5. The exposure began after fish reached 2 months of age in order to allow complete sex determination (Nakamura and Nakahama, 1985; Nakamura et al., 1993; Hines et al., 1999).

Preparation of M. macrocarpa crude extract

Whole stems and tubers of *M. macrocarpa* were ground and dried. The plant powder was extracted with absolute ethanol at room temperature for 2 weeks. Solvent extraction ratio was 1:10, powder (g): solvent (ml). The solution was filtered and the solvent was evaporated out by a rotary evaporator at 40°C at the Natural Products Research Unit, Department of Chemistry, Chulalongkorn University. The crude extract was dried in an oven at 40°C. The extraction process gave approximately 1.51% yield. All crude extracts yielded from each extraction process were pooled together before use in order to minimize variation in chemical composition between each batch.

Subchronic exposure

After the fish reached the age of 2 months, they were separated into 4 aquaria with 300 fish/aquarium. Two aquaria were assigned as the treatment group and the

remaining aquaria were assigned as the control and the solvent control groups. The treatment aquaria were filled with 200 litres of *M. macrocarpa* crude extract solution dissolved in dimethyl sulfoxide (DMSO) at the subchronic concentration of 14 ppm. The control aquarium was filled with 200 litres holding water, and solvent control aquarium was filled with 200 litres of DMSO solution at 20 ppm. The static renewal system was used throughout the experiment and the holding water of every aquarium was renewed every 4 days. The exposure was carried out continuously for seven months. During the exposure period, fish of every aquarium were sampled (n=20) every month from 4 to 7 months after exposure.

Histology

The ovaries were fixed in 10% neutral buffered formalin and processed through standard histological technique for paraffin section (Humason, 1979). All tissue blocks were sectioned at 5 μm and stained with hematoxylin and eosin. Histological structure in the gonad was observed by light microscopy (Zeiss Axioskop 40) comparing between the control and the treated groups.

Activity of 3β-hydroxy steroid dehydrogenase

Steroidogenic potential of the gonad was evaluated using the activity of 3β-hydroxysteroid dehydrogenase (3β-HSD) as a marker. Frozen gonadal tissues were sectioned at 20 μm using a cryostat microtome (Leica CM1850) at -20°C and mounted on poly-l-lysine coated coverslips. Histochemical localization of 3β-HSD was performed according to the procedure modified from Levy et al. (1959). The frozen

sections were incubated at 37°C in phosphate buffer (pH 7.3) containing dehydroepiandrosterone (DHEA, 0.06 mg/ml), nicotinamide adenine dinucleotide (NAD, 0.67 mg/ml) and nitroblue tetrazolium (0.28 mg/ml) for 2 hours. Sections were then fixed in 10% alcoholic formalin, dehydrated, cleared and mounted with DPX. Enzymatic activity in the tissues was visualized as a blue deposit of formazan compound which was further evaluated by scoring method (van den Hurk, 1973; van den Hurk and Peute, 1979; Kang et al., 1995). The enzyme activity was scored by an estimation of the active interlobular/follicular wall area per total interlobular/follicular wall area of the testis/ovary. The scores were classified into 5 levels including: 0 = no activity; 1 = show activity in less than 20% of total interlobular/follicular wall area; 2 = show activity in 50% of total interlobular/follicular wall area; 3 = show activity in 80% of total interlobular/follicular wall area; and 4 = show activity in every interlobular/ follicular wall area. The adjacent frozen sections of every gonad were processed and stained by H&E, and used for histological examination.

Ultrastructure

Twenty four testes (3 testes from control and 3 testes from treated groups of each sampling month) and sixteen ovaries (2 ovaries from control and 2 ovaries from treated groups of each sampling month) were sampled and fixed in 4% glutaraldehyde at 4 °C and post-fixed in 2% osmium tetroxide, and then processed through steps in the rapid protocol for TEM processing (Rowden and Lewis, 1974). Semi-thin sections (150-200 nm) were cut with an ultramicrotome (RMC MT-XL), stained with 0.5 % toluidine blue and observed by light microscopy. From 24 semi-thin testis samples and 16 semi-thin ovary samples, 8 samples were selected from each sex as representatives of

every month and processed for thin sections. Thin sections (90-100 nm) were stained with lead citrate and uranyl acetate and were examined with transmission electron microscope (Jeol JEM-2010) at the Department of Biology, Boston University.

RESULTS

Histology

Cluster of Leydig cells located in the interlobular area in fish testis are shown in Figure 5-1. Histological observation revealed difference in the amount of Leydig cells found in the interlobular area between the control and the treated groups in the early period of experiment. At 4 months post-exposure, large clusters of Leydig cells were found in several individuals of the control group whereas the clusters found in every individual of the treated group were small and shrinked (Figure 5-1A-B). At 5 months post-exposure, large clusters of Leydig cells were found in a half of individuals of the control group whereas every individual of the treated group had large clusters of Leydig cells in their interlobular area of testis (Figure 5-1C-D). After 6 months post-exposure, there was no difference in the amount of Leydig cells found in both groups. Large clusters of Leydig cells were found in a half of individuals in both groups at 6 months post-exposure (Figure 5-1E-F) and smaller clusters were found in some individuals of both groups at 7 months post-exposure.

Somatic cells of ovarian follicle include the inner granulosa cell and the outer thecal cell. Histological structure of follicular walls of the control and the treated groups at different stages of development are shown in Figure 5-7. At light microscopic level, histological structure of the follicular walls in both groups were similar as shown in Figure 5-7A-B at previtellogenic stage and Figure 5-7E-F at ripe stage. However, histological difference was found in the follicular walls at vitellogenic stage (Figure 5-7C-D). Hypertrophy of granulosa cell layer of vitellogenic oocytes in the treated ovaries were observed during 5 to 6 months post-exposure. There was no difference in structure of thecal cell examined at this level.

Activity of 3β-hydroxysteroid dehydrogenase

A positive reaction for 3β-hydroxysteroid dehydrogenase (3β-HSD) activity was indicated by a dark blue deposit of formazan compound as shown in Figure 5-2D and 5-8D. Positive reactions for 3β-HSD were observed in the Leydig cells located in the interlobular area in the testes and the interstitial cell and thecal cell in the ovaries of the tilapia. These activities were specific to only cytoplasmic compartment of the positive cells.

Histochemical detection of 3β-HSD activity in the tilapia testes was scored and shown in Table 5-1. The 3β-HSD activity was found at similar levels (2.33-2.75 scores) in the testes of the control group during 4 to 6 months post-exposure (Figure 5-2E, 5-3A and 5-3C) and then the activity decreased at 7 months post-exposure (Figure 5-3E). In the treated group, activity of the enzyme was observed at low level (1.14 scores) at 4 months post-exposure (Figure 5-2F) and then increased to the highest level (3.25 scores) at 5 months post-exposure (Figure 5-3B). At 6 months post-exposure, the enzyme activity in the treated group was at the same level as that of the control (Figure 5-3D) and then decreased at 7 months post-exposure similar to the control (Figure 5-3F).

Histochemical detection of 3β-HSD activity in the tilapia ovaries was scored and shown in Table 5-2. In the follicular wall, the positive enzymatic activity was found in thecal cell layer (Figure 5-8D) and interstitial cells in some interfollicular area of the ovary. The 3β-HSD activity was found at high level (3.0 score) in the ovaries of the control group at 4 months post-exposure (Figure 5-8E), then the activity decreased to moderate level (2.33 score) at 6 months post-exposure (Figure 5-9C) and low level (1.75 score) at 7 months post-exposure (Figure 5-9E). In the treated group, activity of

the enzyme was observed in moderate level (2.50 score) at 4 months post-exposure (Figure 5-8F) and increased to high level (3.0 score) at 5 months post-exposure (Figure 5-9A-B). Then at 6 to 7 months post-exposure, activity of the enzyme was observed at moderate level (2.33-2.00 score, respectively) (Figure 5-9D and 5-9F).

Ultrastructural markers of steroidogenesis

Ultrastructure of steroid producing cells of the tilapia gonad was examined according to the morphological criteria for steroid producing cells by Pudney (1987) as stated below. An active steroid producing cell possesses abundant cytoplasm and a regular spherical nucleus with finely dispersed chromatin and peripheral clumps of heterochromatin located adjacent to the nuclear membrane. An inactive steroid producing cell has reduced volume of cytoplasm and an irregular-shaped nucleus with increased amounts of heterochromatin. General cytological appearance of the steroid producing cells includes the presence of an extensive smooth endoplasmic reticulum, mitochondria with various inclusions (e.g. lipids) and tubulovesicular cristae (tubular in long section and vesicular in cross section), lipid droplets, lipofuscin granules and filaments.

Leydig cells were found in the interlobular area of the testis. They grouped as a cluster in association with blood capillaries as shown in Figure 5-4A. At 4 months post-exposure, inactive Leydig cells were found in both control and treated groups (Figure 5-4A-B). The inactive Leydig cell of the tilapia possessed an irregular-shaped nucleus with heterochromatin and cytoplasm with electron-dense vesicles and smooth endoplasmic reticulum (Figure 5-4C). Some active Leydig cells were found in the treated group at this period. They contained a regular spherical nucleus with peripheral

clumps of heterochromatin and one distinct nucleolus (Figure 5-4D). Their cytoplasm contained abundant mitochondria and smooth endoplasmic reticulum. After 5 months post-exposure, active Leydig cells were found in the testes of both groups. Ultrastructures of these active Leydig cells of the control and the treated groups were similar as shown in Figure 5-5 and 5-6. They possessed a spherical nucleus with one distinct nucleolus and cytoplasm with abundant mitochondria and smooth endoplasmic reticulum. The mitochondria contained electron-dense inclusions (Figure 5-5B-C and 5-6B-C) and tubulovesicular cristae (Figure 5-5D and 5-6D). The smooth endoplasmic reticulum was generally found in globular form (Figure 5-5D and 5-6D).

In female fish, both granulosa cell and thecal cell were reported to involve in gonadal steroidogenesis as reviewed by Guraya (1976). However, ultrastructural features of the tilapia granulosa cells in this study did not indicate an active steroidogenesis in most stages examined. The granulosa cell of early stage oocyte (perinucleolar and cortical alveolar stages) of the control and the treated groups were similar. They contained small amount of cytoplasm with free ribosomes, tubular rough endoplasmic reticulum, well developed Golgi system and some mitochondria (Figure 5-10A-B and 5-11A-B). Electron-dense materials were found firstly in the cortical alveolar stage (Figure 5-10B and 5-11B). In vitellogenic stage, granulosa cells of the control group were found in an active state of protein secreting cell. They contained cytoplasm with extensive tubular rough endoplasmic reticulum, free ribosomes, mitochondria and electron-dense materials (Figure 5-10C). The granulosa cells at vitellogenic stage in the treated group were found to be hypertrophied. Nucleus and organelles including structurally normal mitochondria, rough endoplasmic reticulum and some electron-dense vesicles were packed at the periphery (Figure 5-11C), whereas

the other area was filled with membranous debris, fat droplets and autophagic vacuoles. At ripe stage, the granulosa cells of the control group possessed abundant mitochondria, tubular rough endoplasmic reticulum and free ribosomes (Figure 5-10D), but no smooth endoplasmic reticulum was found. In contrast, the granulosa cells of the treated group at this stage contained some smooth endoplasmic reticulum, mitochondria and several vesicles with electron-dense content and lipid-like content (Figure 5-11D), possibly indicate a steroidogenic activity.

The thecal cells at early to vitellogenic stages of the control group were found to be actively steroidogenic with abundant smooth endoplasmic reticulum as shown in Figure 5-12. At vitellogenic stage, the thecal cells contained abundant mitochondria with electron-lucent content and tubulovesicular cristae (Figure 5-12C). Pleomorphic mitochondria with electron-dense and filamentous inclusions were also found (Figure 5-12 inset). In the treated group, the thecal cells at early stage were also active with abundant mitochondria with tubulovesicular cristae and smooth endoplasmic reticulum (Figure 5-13A). But, at cortical alveolar stage, some thecal cells were atrophied with the presence of large electron-dense vesicles, dilated endoplasmic reticulum and myelin figures (Figure 5-13B). At vitellogenic stage, the thecal cells of the treated group were found to be steroidogenically active with abundant smooth endoplasmic reticulum and mitochondria with tubulovesicular cristae (Figure 5-13C).

DISCUSSION

In this study, histochemical and ultrastructural endpoints were used to assess potential effects of *M. macrocarpa* crude extract on gonadal steroidogenesis in the tilapia. Histological observation by light microscopy revealed some differences in size of Leydig cell cluster between the control and the treated groups during 4 to 5 months post-exposure. Large size of the cluster may indicate proliferation and/or active state of the Leydig cells. Therefore, the small Leydig cell clusters found in the treated group at 4 months post-exposure may imply that Leydig cells were nonproliferative/inactive at this period and then became proliferative/active at 5 months post-exposure. Whereas the control Leydig cells were found to be proliferative/active since 4 months post-exposure. In the females, most of histological structure of the follicular wall was not different between groups, except the marked hypertrophy of granulosa cell layer of the vitellogenic oocytes in the treated group. This may indicate a histopathological alteration within this cell. However in some studies, hypertrophy of granulosa cell was discussed as a normal incidence and/or an active state under gonadotropin stimulation (Rosenblum et al., 1987; Nakamura et al., 1993; Sundararaj et al., 1972).

The presence of 3β-HSD activity in the tilapia gonads indicates their potential steroidogenic function. The activity of 3β-HSD and the ultrastructure of the steroid producing cells are well correlated (Guraya, 1976; Schreibman et al., 1982). These two markers are thus discussed together in this study.

Testicular steroidogenesis

In this study, the 3β-HSD activity of the control fish seemed to be constant during 4 to 6 months and then dropped at 7 months post-exposure. Based on the studies

focusing on steroid-producing cells of *O. niloticus,* Leydig cells with active steroidogenic features appeared initially at the onset of testicular differentiation and increased in number rapidly after 70 days post hatch (Nakamura and Nagahama, 1989). Therefore the steroidogenic potential of every fish used in this study (6-9 months post hatch) should be in an active state. However, comparison of 3β-HSD activity revealed differences in testicular steroidogenic function between the control and the treated groups. In correlation with the result from histological observation, the activity of 3β-HSD in the treated group was low at 4 months post-exposure and peaked at 5 months post-exposure, then dropped to the levels similar to that of the control in the later period. The reduced activity of the treated Leydig cells at 4 months post-exposure compared to the control may indicate a delayed in steroidogenic potential due to a suppressive effect of *M. macrocarpa* extract. Then, the steroidogenesis in the treated testes was corrected by 5 months post-exposure as seen by a markedly increased activity, and became similar to the control at 6-7 months post-exposure suggesting that the steroidogenic functions were not altered by the treatment after prolonged period. The suppressive effect of this plant extract on steroidogenesis in Leydig cells is correlated with the properties of its chemical constituent, quercetin. Quercetin can increase physiological concentration of tumor necrosis factor alpha (TNF-α) in murine lymphocytic cells (Orzecchowski et al., 2000). An elevated TNF-α has an inhibitory role in the steroidogenesis of Leydig cells at the level of gene expression of various steroidogenic enzymes including 3β-HSD (Hong et al., 2004).

The ultrastructural features of steroidogenesis found in the tilapia Leydig cell are similar to those reported in another cichlid fish, *Cichlasoma nigrofasciatum*, by

Nicholls and Graham (1972). As seen in fish at 7 months post-exposure when the 3β-HSD activity was minimal but the ultrastructural features indicated high steroidogenic activity, the result from this study indicates that the ultrastructural study may provide a more sensitive detection of steroidogenesis in the tilapia testis than the histochemical method. Similar observation was also reported by Gresik et al. (1973) in the study of *Oryzias latipes*, in which the Leydig cells of the fish showed negative 3β-HSD activity whereas their ultrastructure showed active steroidogenesis. This finding suggests that eventhough 3β-HSD activity is a key biomarker for steroidogenesis in Leydig cell, it is crucial to confirm the result with the ultrastructural study.

Ovarian steroidogenesis

In the females, 3β-HSD activity in the ovaries of the control group was gradually decreased from high activity at 4 months post-exposure to low activity at 7 months post-exposure. In the treated females, moderate activity was observed at 4 months post-exposure and then increased to high activity at 5 months post-exposure. After that, the enzymatic activity seemed to be similarly decreased in both groups. Similar to the males, the treated ovaries also showed a suppressive activity at 4 months post-exposure and a corrected activity at 5 months post-exposure, and became similar to the control in later period. Similar effect of plant extract on ovarian steroidogenesis has been reported. The treatment of *Cuscuta reflexa*, a medicinal plant contained large quantity of flavonoids, and *Corchorus olitorius*, a medicinal plant contained cardenolide glycosides, results in a significant reduction of 3β-HSD activity in adult female mice (Gupta et al., 2003).

It is of interest to note that 3β-HSD activity found in this study was specific to the interstitial cells and the thecal cells of the ovarian follicle whereas no activity was found in the granulosa cells. This different degree of steroidogenic potential within the ovarian follicular compartments seems to be varied among taxa. The study on 3β-HSD activity in the ovary of mackerel, *Scomber scomber*, showed that activity was specific to the thecal cells and strongest at the beginning of vitellogenesis, and became reduced as the follicle matured (Bara, 1965 cited in Guraya, 1976), which is similar to the result of this study. A similar result was also reported in the study in platyfish, *Xiphophorus maculatus* ovary (Schreibman et al., 1982). In contrast, positive 3β-HSD activity was reported in granulosa cells of catfish, *Mystus vittatus* ovarian follicle (Upadhyaya and Haider, 1985).

The result from ultrastructural study also confirms lack of steroidogenic features in the granulosa cells. But the exception was found in the treated group at ripe stage. The presence of smooth endoplasmic reticulum and several vesicles, especially lipid vesicles, in the treated granulosa cells may indicate steroidogenesis. As also reported in two cichlid fish, *Cichlasoma nigrofasciatum* and *Haplochromis multicolor*, evidence of steroidogenesis in the granulosa cells was the presence of transport vesicles (Nicholls and Maple, 1972). It is known that granulosa and thecal cells play different roles in two-cell hypothesis of steroidogenesis (Young et al., 1986; Nagahama, 1997). The thecal cell is behaved to produce steroid precursors (androgens) and the granulosa cell converts androgens to estradiol-17β or other steroid mediators (Nagahama, 1988; Khan and Thomas, 1999; Devlin and Nagahama, 2002). The results from this study suggest that thecal cell of this species has steroidogenic capacity. The granulosa cells possess organelles typical of protein-secreting cells suggesting additional functions in synthesis

of the envelope. Similar results have also been reported in marine teleosts such as the mackerel *Scomber scomber*, zebra fish *Brachydanio rerio* and red sea bream *Pagrus major* (Bara, 1965, Yamamoto and Onozato 1968 cited in Guraya, 1976; Matsuyama et al., 1991). The protein-secreting character of the granulosa cell correlates with the fact that there is high production of enzymes involved in the conversion of steroid precursors (Guraya, 1986).

The thecal cells of the tilapia show active steroidogenic features at all stages in the control group with mitochondria-rich character at vitellogenic stage. The presence of pleomorphic mitochondria with electron-dense and filamentous inclusions is also a character of active steroidogenic cell and also reported in thecal cells of cichlid fish (Nicholls and Maple, 1972) and in Leydig cells of medaka (Gresik et al., 1973). It is of importance to note some atrophied thecal cells with the presence of large electron-dense vesicles, dilated endoplasmic reticulum and myelin figures in the treated fish at previtellogenic stage, which may indicate an alteration in steroidogenic function of the thecal cells. Based on the histochemical detection of 3β-HSD activity and ultrastructural study in rainbow trout, *Salmo gairdneri*, ovarian steroidogenesis was found throughout the cycle and reached a peak activity during the period of ovulation and previtellogenesis (van den Hurk and Peute, 1979). Therefore, the atrophy of thecal cells at previtellogenic stage in the treated fish should not be regarded as a normal incidence.

The present study examined the effects of *M. macrocarpa*, a plant used in traditional remedy for treating male sexual dysfunction and containing several hormonally active ingredients. Overall results from subchronic treatment on the tilapia

showed several alterations of gonadal steroidogenic function. Histochemical result showed that testicular steroidogenesis may be delayed by the treatment of the plant extract. In females, lack of steroidogenic activity of the thecal cells implies that ovarian steroidogenesis in previtellogenic stage may be altered by the treatment of the plant extract.

TABLES AND FIGURES

Table 5-1: Activity of 3β-Hydroxy steroid dehydrogenase in *O. niloticus* testes after exposure to the crude extract from *M. macrocarpa*. Score: 0 = no activity; 1 = show activity in less than 20% of total interlobular area; 2 = show activity in 50% of total interlobular area; 3 = show activity in 80% of total interlobular area; and 4 = show activity in every interlobular area.

Months after exposure	Average score	
	Control	Treatment
4	2.43	1.14
5	2.33	3.25
6	2.75	2.67
7	1.00	0.67

Table 5-2: Activity of 3β-Hydroxy steroid dehydrogenase in *O. niloticus* ovaries after exposure to the crude extract from *M. macrocarpa*. Score: 0 = no activity; 1 = show activity in less than 20% of total follicular wall area; 2 = show activity in 50% of total follicular wall area; 3 = show activity in 80% of total follicular wall area; and 4 = show activity in every follicular wall area.

Months after exposure	Average score	
	Control	Treatment
4	3.00	2.50
5	(no sample)	3.00
6	2.33	2.33
7	1.75	2.00

Figure 5-1: Light micrograph of *O. niloticus* testes shows Leydig cells in the interlobular spaces. (A) The control testis with large clusters of Leydig cells (arrows) and (B) the treated testis with small shrinked clusters of Leydig cells (arrows) at 4 months post-exposure. (C) The control testis and (D) the treated testis at 5 months post-exposure both with large clusters of Leydig cells (*). (E) The control testis and (F) the treated testis at 6 months post-exposure both with large clusters of Leydig cells (*). *Bar*: 20 μm. *H&E stain.*

S seminiferous lobule.

Figure 5-1

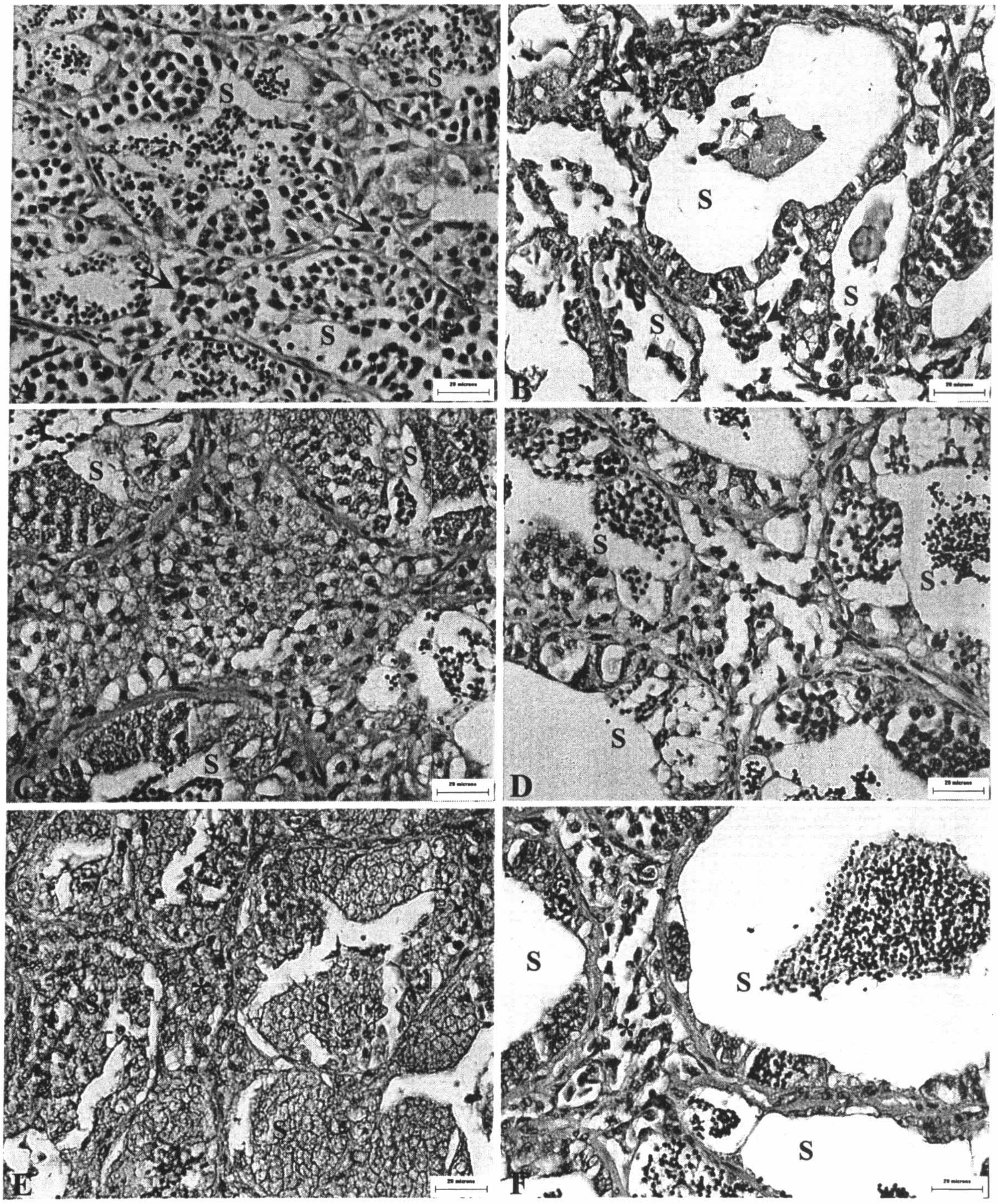

Figure 5-2: Histochemical detection of 3β-hydroxy steroid dehydrogenase (3β-HSD) activity in testes of *O. niloticus* at 4 months post-exposure. (A) Normal testis of the control fish at low magnification. *Bar*: 150 μm. *H&E stain*. (B) The control testis at high magnification shows Leydig cells (arrow) in the interlobular space (dotted square). *Bar*: 20 μm. *H&E stain*. (C) The control testis in the section paralleled with (A) shows positive 3β-HSD activity. *Bar*: 150 μm. (D) The positive 3β-HSD activity in the control testis section paralleled with (B). The activity was observed as dark blue formazan deposits in cytoplasm of the Leydig cells (arrow). *Bar*: 20 μm. (E) The control testis shows positive 3β-HSD activity in interlobular spaces. *Bar*: 80 μm. (F) The testis of the treated fish shows negative 3β-HSD activity. *Bar*: 80 μm.

S seminiferous lobule.

Figure 5-2

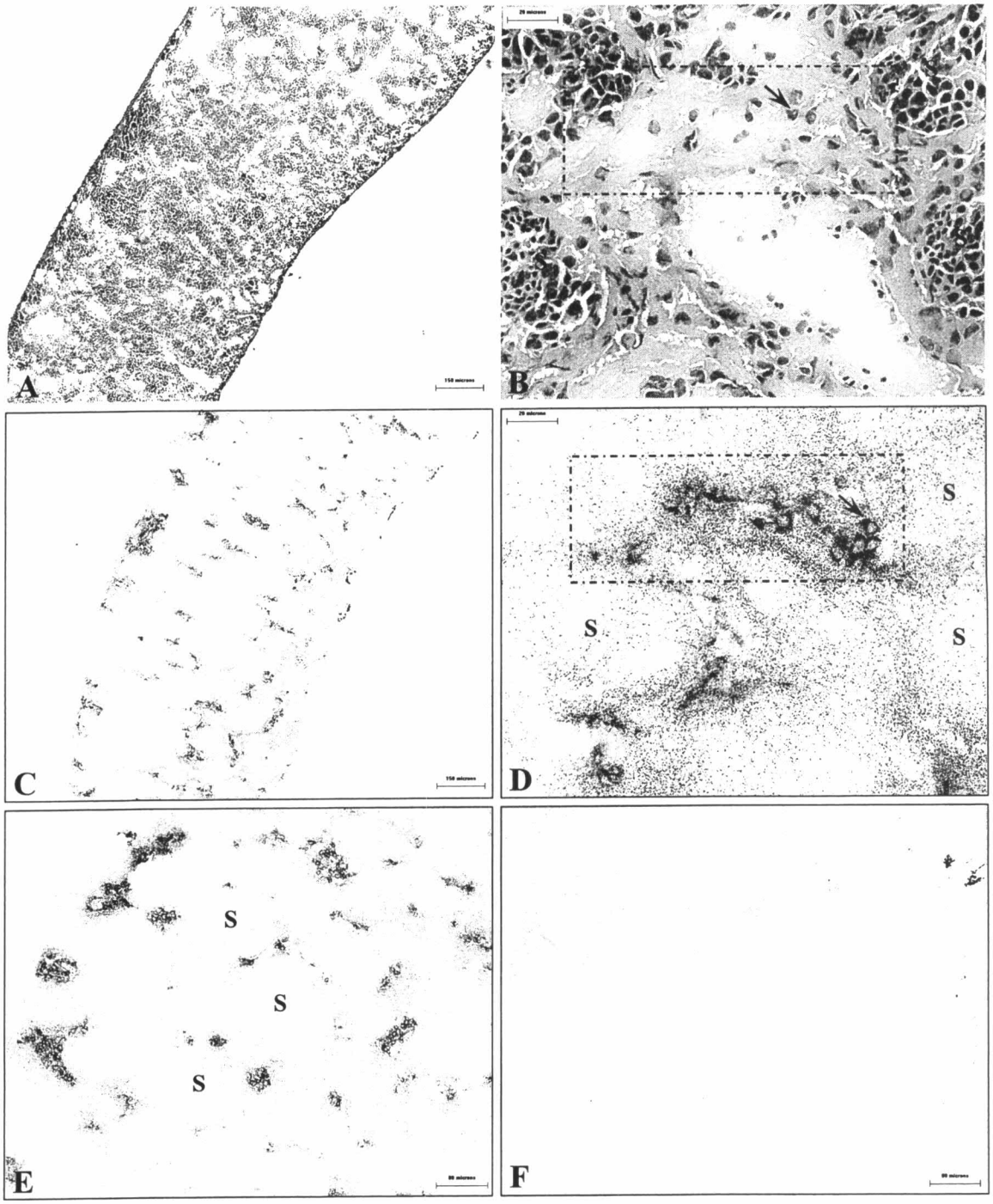

Figure 5-3: Histochemical detection of 3β-hydroxy steroid dehydrogenase (3β-HSD) activity in testes of *O. niloticus*. (A) The testis of the control fish at 5 months post-exposure shows high activity of 3β-HSD (arrows) in the interlobular spaces. *Bar*: 80 μm. (B) The testis of the treated fish at 5 months post-exposure also shows high activity of 3β-HSD (arrows). *Bar*: 80 μm. (C) The testis of the control fish at 6 months post-exposure shows moderate activity of 3β-HSD (arrows) in the interlobular spaces. *Bar*: 80 μm. (D) The testis of the treated fish at 6 months post-exposure shows similarly moderate activity of 3β-HSD (arrows). *Bar*: 80 μm. (E) The testis of the control fish at 7 months post-exposure shows low activity of 3β-HSD (arrows) in the interlobular spaces. *Bar*: 80 μm. (F) The testis of the treated fish at 7 months post-exposure shows low activity of 3β-HSD (arrows) as well. *Bar*: 80 μm.

S seminiferous lobule.

Figure 5-3

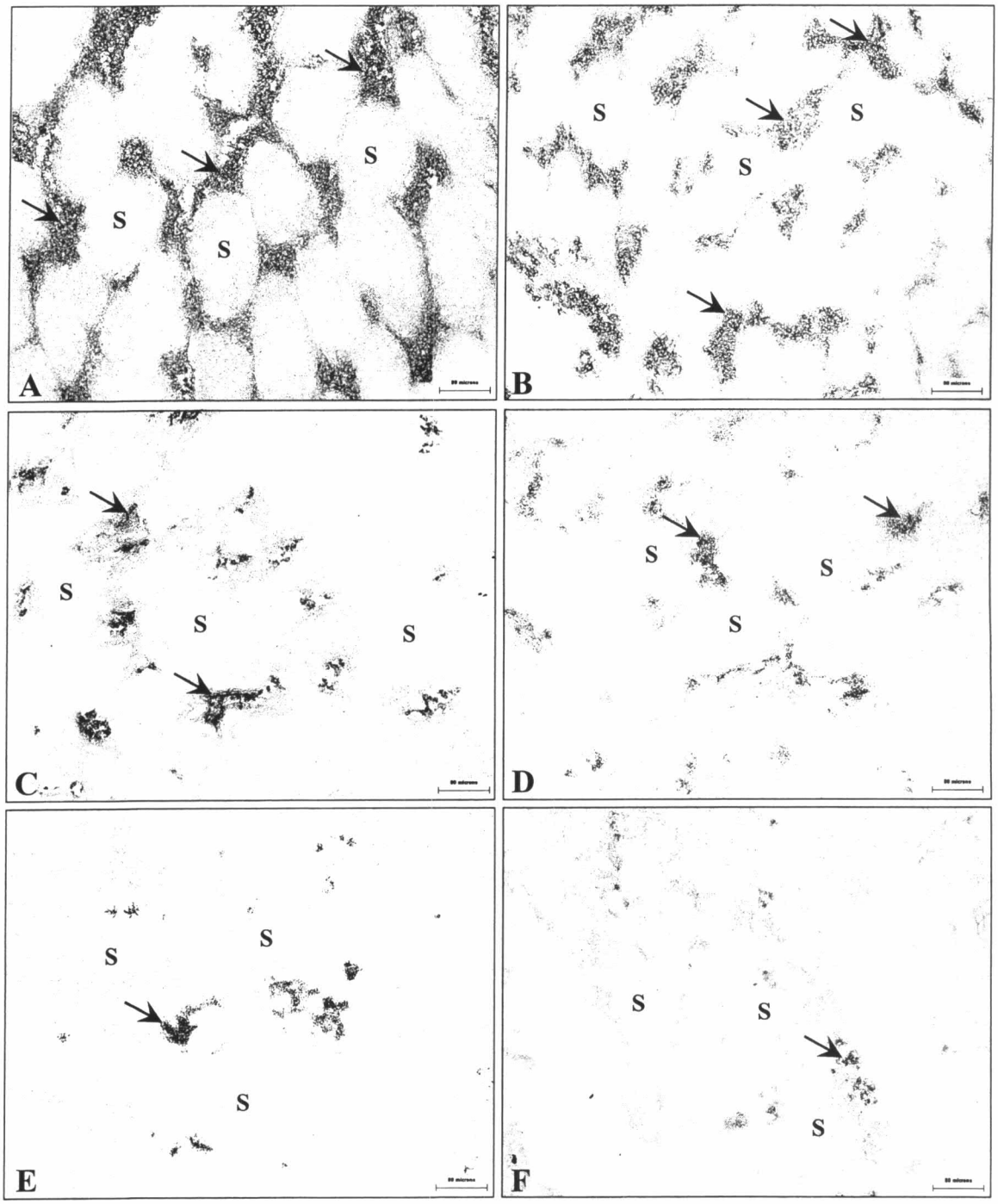

Figure 5-4: Electron micrograph of Leydig cells of *O. niloticus* at 4 months post exposure. (A) Cluster of inactive Leydig cells of the control fish. ×3,000. *Bar*: 1 μm. (B) Cluster of inactive Leydig cells of the treated fish. ×6,000. *Bar*: 1 μm. (C) An inactive Leydig cell of the control fish at high magnification shows irregular-shaped nucleus with large amount of heterochromatin and cytoplasm with electron-dense vesicles. ×15,000. *Bar*: 500 nm. (D) An active Leydig cell of the treated fish at high magnification shows spherical nucleus with one nucleolus and peripheral clumps of heterochromatin adjacent to the nuclear membrane and cytoplasm with abundant mitochondria and SER (arrows). ×20,000. *Bar*: 200 nm.

C blood capillary, *L* Leydig cell, *Lb* lobule boundary cell, *N* nucleus, *m* mitochondria, *S* seminiferous lobule, *v* vesicles.

Figure 5-4

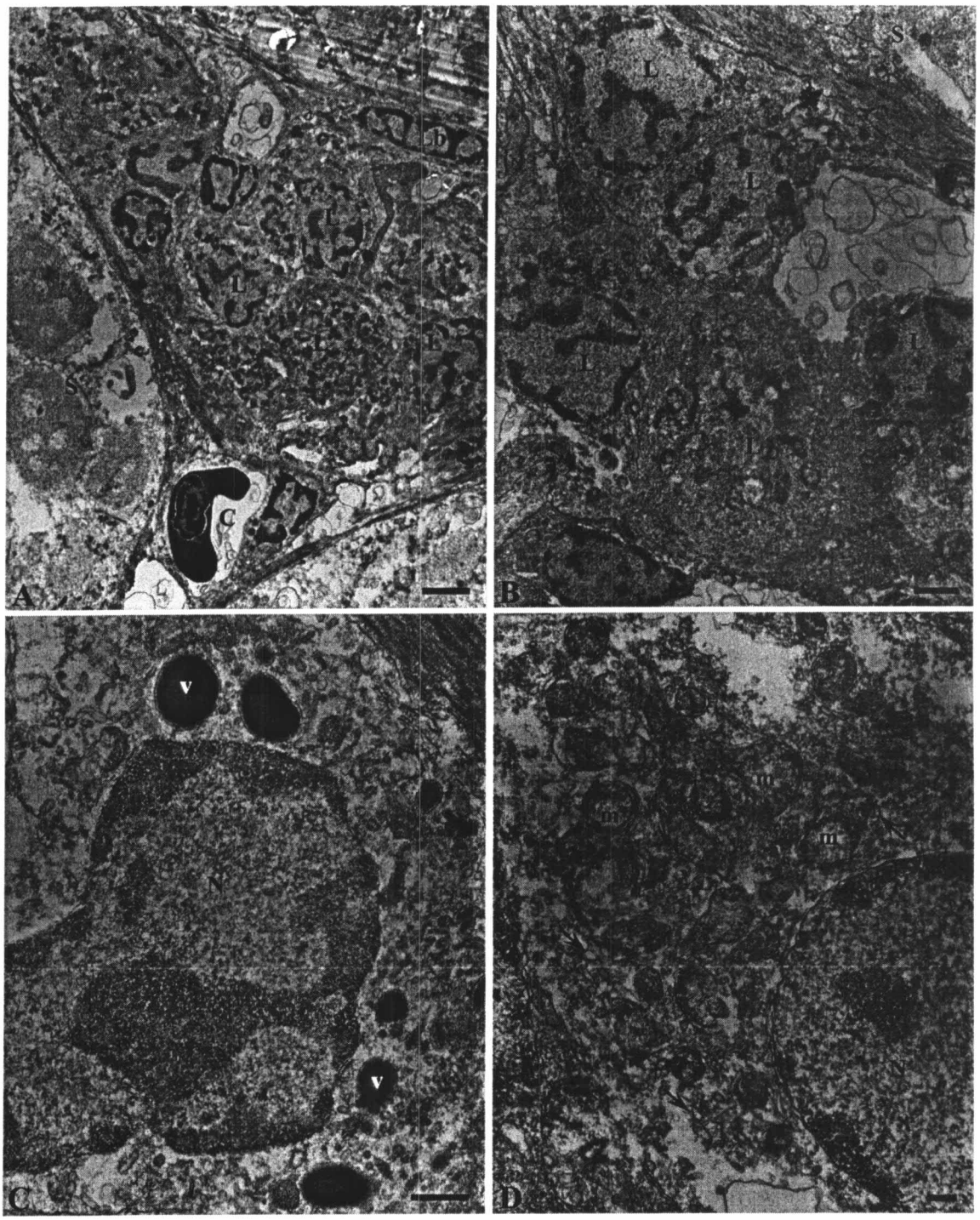

Figure 5-5: Electron micrograph of Leydig cells of the control *O. niloticus*. (A) Low magnification of cluster of active Leydig cells at 5 months post-exposure contain nucleus with euchromatin (*). ×5,000. *Bar*: 1 μm. (B) An active Leydig cell at 5 months post-exposure shows abundant globular SER (arrows) and mitochondria with electron-dense matrix and tubulovesicular cristae. ×20,000. *Bar*: 200 nm. (C) An active Leydig cell at 6 months post-exposure shows abundant mitochondria with electron-dense matrix. ×20,000. *Bar*: 200 nm. (D) An active Leydig cell at 7 months post-exposure also shows abundant mitochondria with electron-dense matrix and globular SER (arrows). ×20,000. *Bar*: 200 nm.

L Leydig cell, *N* nucleus, *m* mitochondria.

Figure 5-5

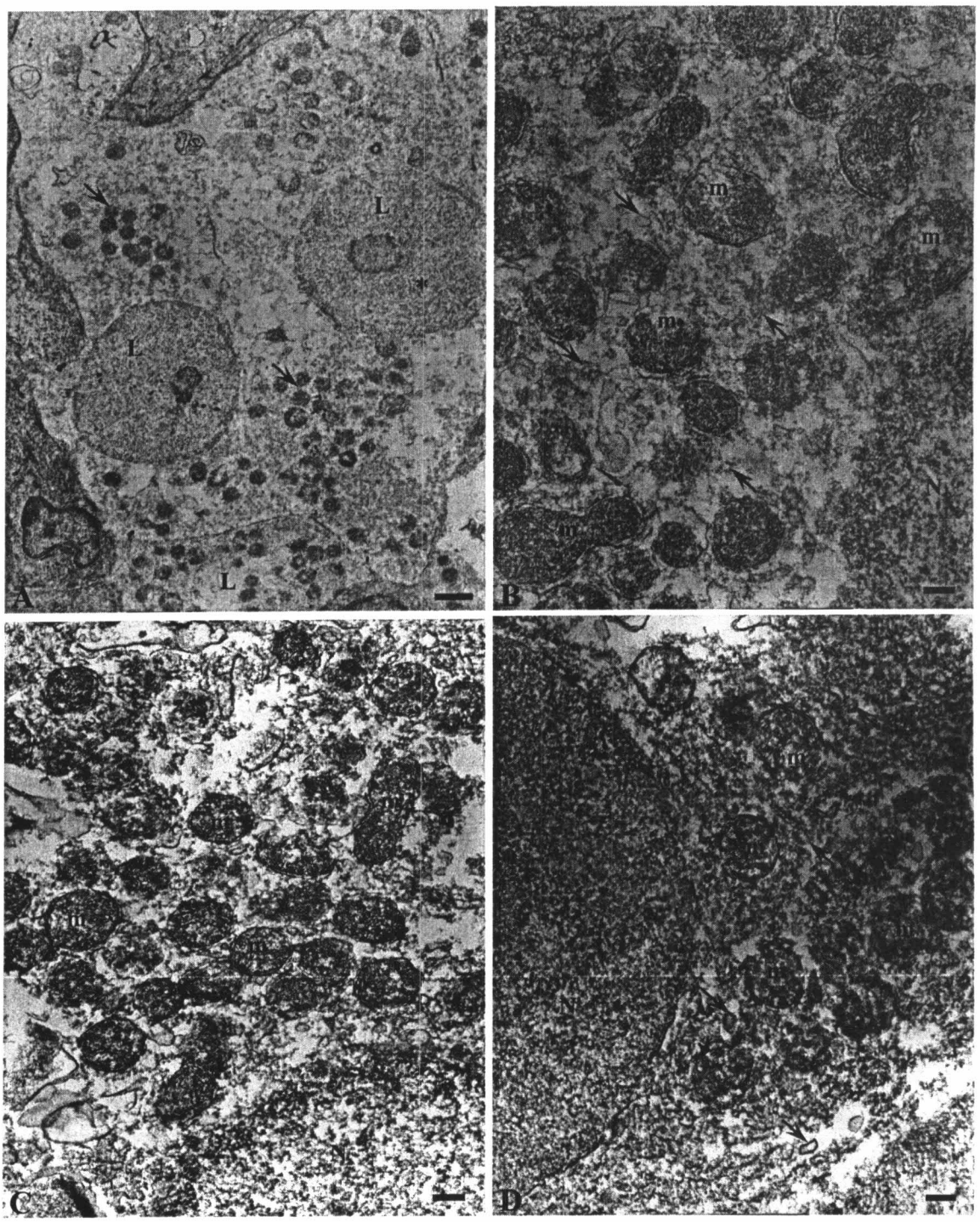

Figure 5-6: Electron micrograph of Leydig cells of the treated *O. niloticus*. (A) Low magnification of cluster of active Leydig cells at 6 months post-exposure contain nucleus with euchromatin (*) and abundant electron-dense mitochondria (arrows). ×5,000. *Bar*: 1 μm. (B) An active Leydig cell at 5 months post-exposure shows abundant globular SER and mitochondria with tubulovesicular cristae. ×20,000. *Bar*: 200 nm. (C) An active Leydig cell at 6 months post-exposure shows abundant mitochondria with electron-dense matrix and globular SER. ×20,000. *Bar*: 200 nm. (D) An active Leydig cell at 7 months post-exposure also shows abundant mitochondria with tubulovesicular cristae and globular SER. ×20,000. *Bar*: 200 nm.

L Leydig cell, *N* nucleus, *m* mitochondria.

Figure 5-6

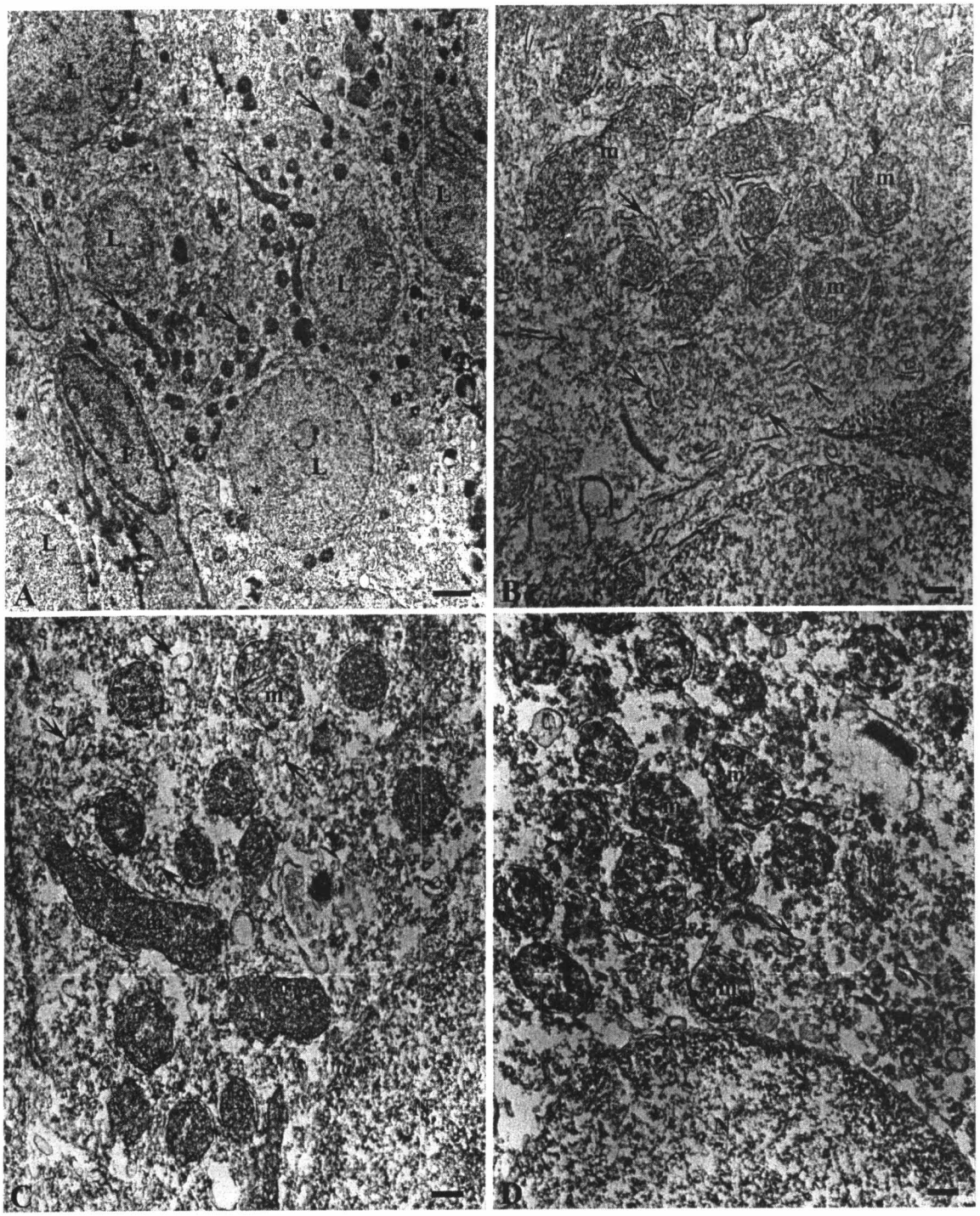

Figure 5-7: Light micrograph of the ovaries of *O. niloticus* shows ovarian follicles at different stages. (A) Follicle of cortical alveolar oocyte of the control group. (B) Follicle of cortical alveolar oocyte of the treated group. (C) Follicle of vitellogenic oocyte of the control group with yolk droplets in granulosa layer. (D) Follicle of vitellogenic oocyte of the treated group with hypertrophy granulosa layer. (E) Follicle of ripe oocyte of the control group. (F) Follicle of ripe oocyte of the treated group. *Bar*: 20 μm. *H&E stain.*

Ca cortical alveolar oocyte, *G* granulosa cell, *L* lipid droplet, *P* perinucleolar oocyte, *R* ripe oocyte, *T* thecal cell, *V* vitellogenic oocyte, *Y* yolk droplet.

Figure 5-7

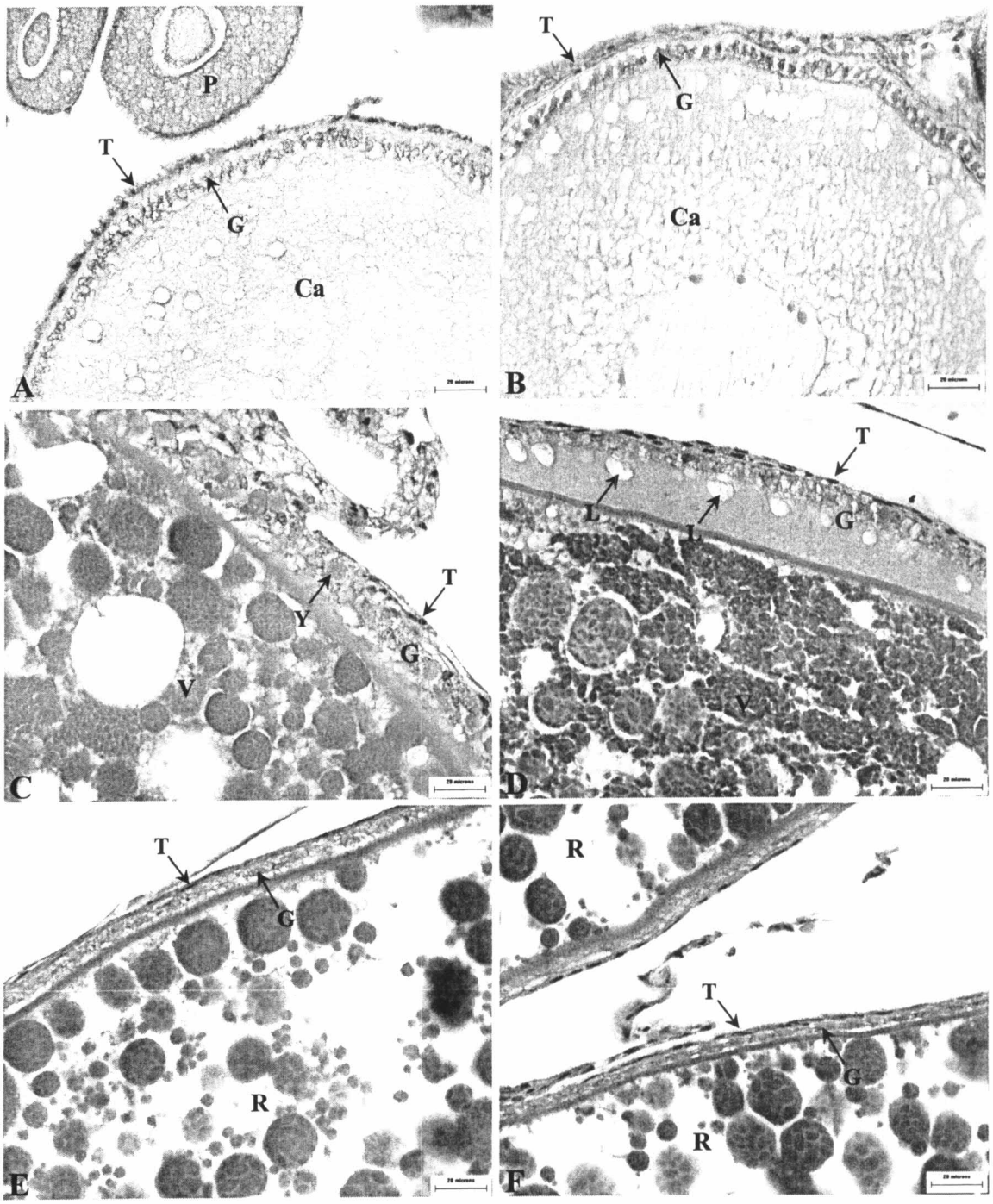

Figure 5-8: Histochemical detection of 3β-hydroxy steroid dehydrogenase (3β-HSD) activity in the ovaries of *O. niloticus* at 4 months post-exposure. (A) Normal ovary of the control fish at low magnification. *Bar*: 150 μm. *H&E stain*. (B) The control ovary at high magnification shows follicle wall consisting of proliferated granulosa cells and thecal cells (arrows). *Bar*: 20 μm. *H&E stain*. (C) The control ovarian section paralleled with (A) shows positive 3β-HSD activity. *Bar*: 150 μm. (D) The positive 3β-HSD activity in thecal cells of the control ovarian section paralleled with (B). The activity was observed as dark blue formazan deposits in cytoplasm of the thecal cells (arrows). *Bar*: 20 μm. (E) The control ovary shows positive 3β-HSD activity (arrows) in the follicle walls and interstitial cells. *Bar*: 80 μm. (F) The ovary of the treated fish shows positive 3β-HSD activity (arrows) in the follicle walls and interstitial cells. *Bar*: 80 μm.

G granulosa cell, *V* vitellogenic oocyte.

Figure 5-8

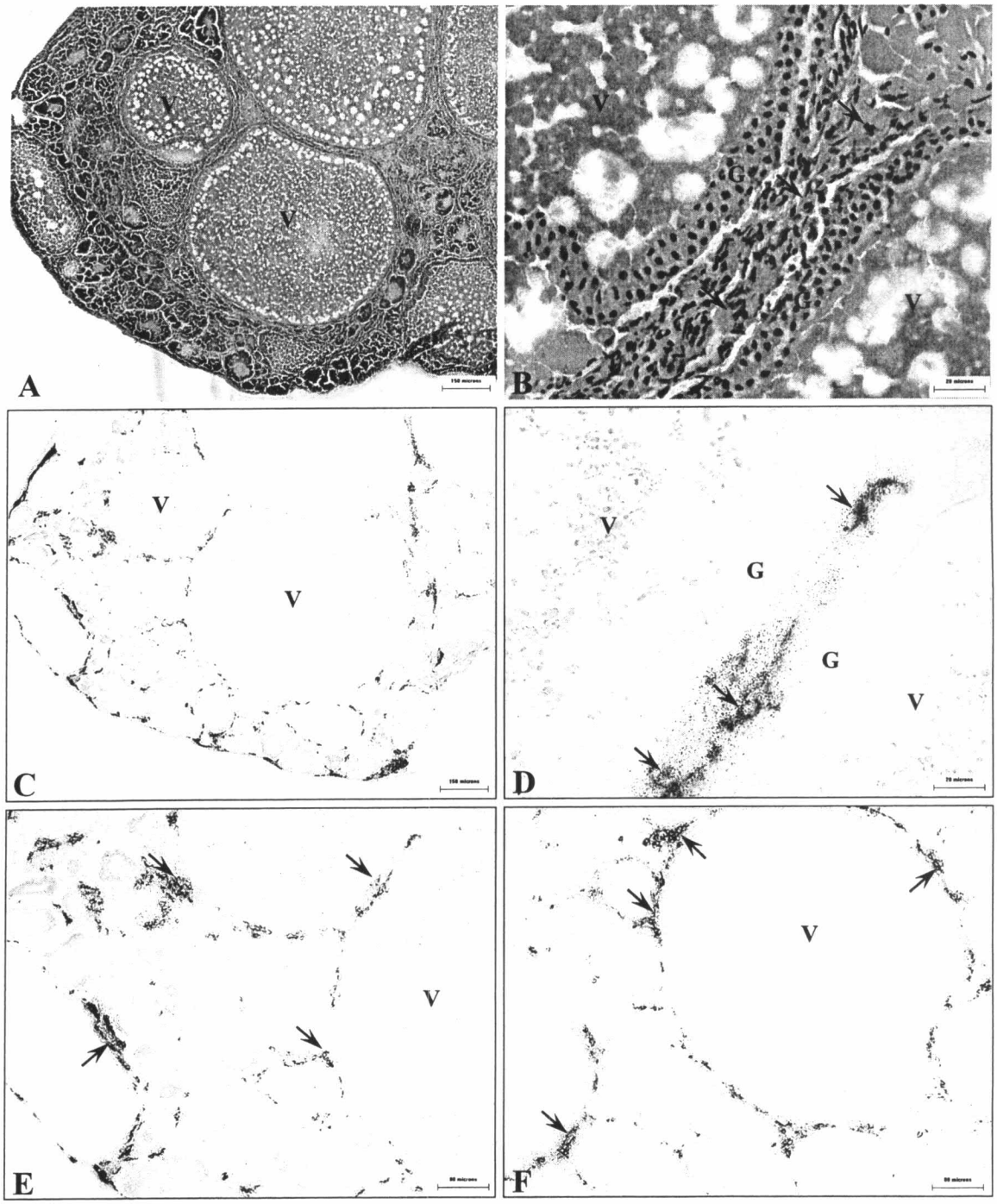

Figure 5-9: Histochemical detection of 3β-hydroxy steroid dehydrogenase (3β-HSD) activity in ovaries of *O. niloticus*. (A) The ovary of the treated fish at 5 months post-exposure shows high activity of 3β-HSD (arrows) in the follicle walls and interstitial cells. *Bar*: 80 μm. (B) High magnification of (A) shows high activity of 3β-HSD (arrows) in thecal cell layer. *Bar*: 20 μm. (C) The ovary of the control fish at 6 months post-exposure shows moderate activity of 3β-HSD (arrows) in the follicle walls and interstitial cells. *Bar*: 80 μm. (D) The ovary of the treated fish at 6 months post-exposure also shows moderate activity of 3β-HSD (arrows) in the follicle walls. *Bar*: 80 μm. (E) The ovary of the control fish at 7 months post-exposure shows moderate activity of 3β-HSD (arrows) in the follicle walls. *Bar*: 80 μm. (F) The ovary of the treated fish at 7 months post-exposure shows similarly moderate activity of 3β-HSD (arrows). *Bar*: 80 μm.

V vitellogenic oocyte, *R* ripe oocyte.

Figure 5-9

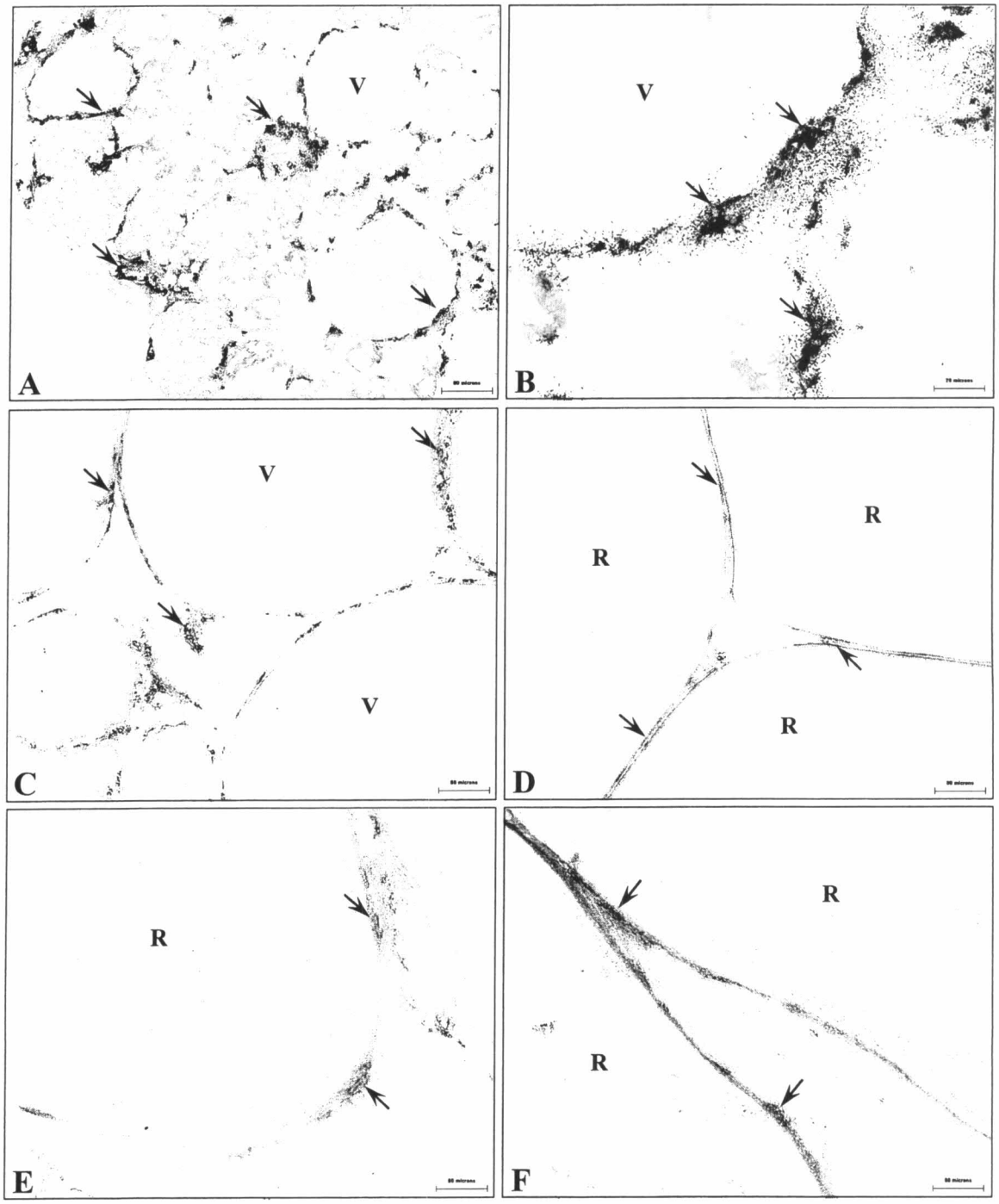

Figure 5-10: Electron micrograph of granulosa cells of the control *O. niloticus*. (A) A granulosa cell of perinucleolar oocyte with free ribosomes (square), tubular RER and multivesicular bodies. ×20,000. *Bar*: 200 nm. (B) A granulosa cell of cortical alveolar oocyte with deposition of some electron-dense material (*) and abundant free ribosomes (square) and tubular RER. ×20,000. *Bar*: 200 nm. (C) A granulosa cell of vitellogenic oocyte with numerous mitochondria, dilated tubular RER, free ribosomes (square) and electron-dense material (*). ×20,000. *Bar*: 200 nm. (D) A granulosa cell of ripe oocyte with abundant elongate mitochondria, tubular RER and free ribosomes (square). ×15,000. *Bar*: 500 nm.

O oocyte, *Bm* basement membrane, *N* nucleus, *RER* rough endoplasmic reticulum, *m* mitochondria, *mvb* multivesicular bodies.

Figure 5-10

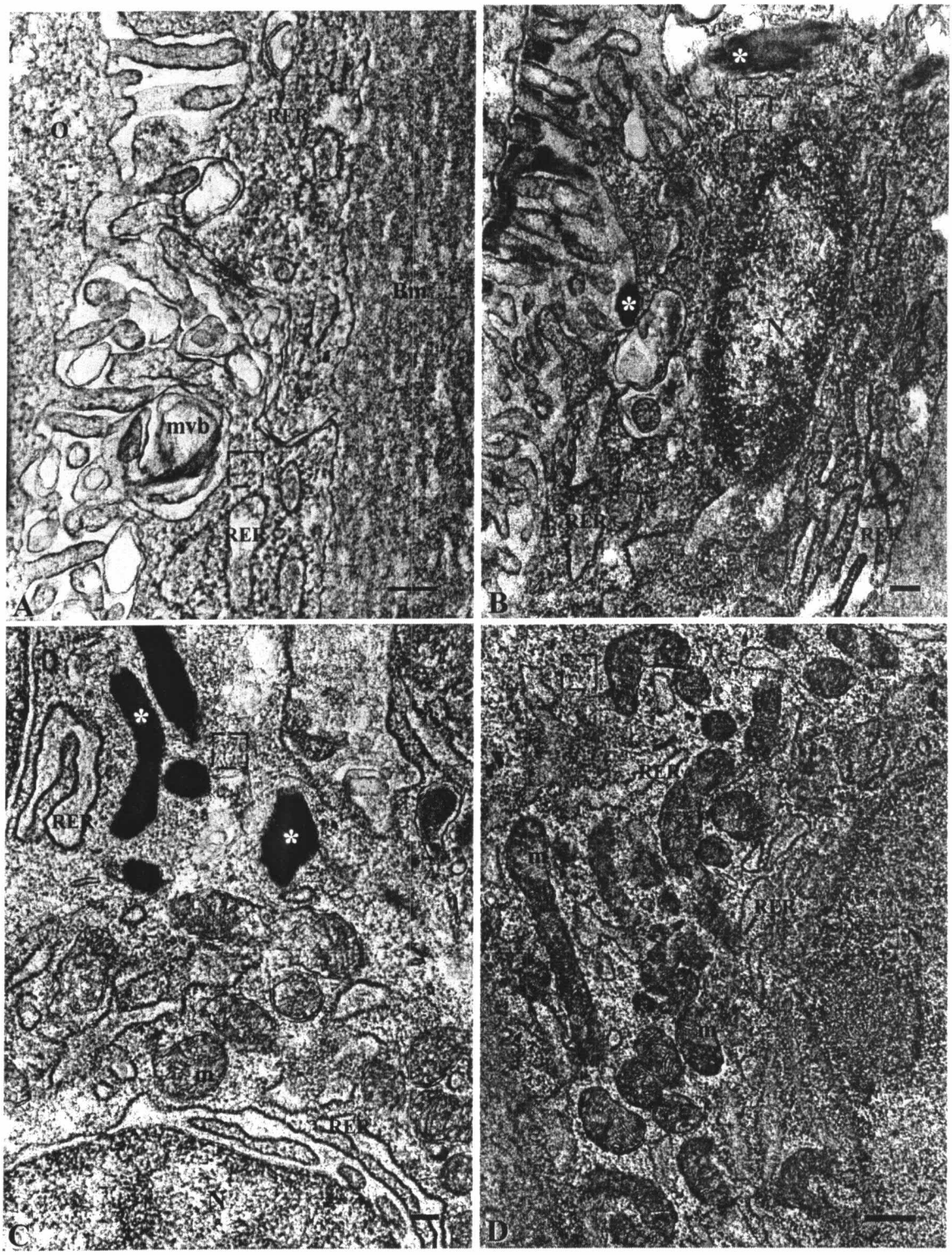

Figure 5-11: Electron micrograph of granulosa cells of the treated *O. niloticus*. (A) A granulosa cell of perinucleolar oocyte. ×20,000. *Bar*: 200 nm. (B) A granulosa cell of cortical alveolar oocyte with well developed Golgi system, RER and deposition of electron-dense material. ×20,000. *Bar*: 200 nm. (C) A granulosa cell of vitellogenic oocyte with hypertrophied granulosa cell layer. All organelles are packed in the periphery near the basement membrane including RER whorl. ×8,000. *Bar*: 1 μm. (D) A granulosa cell of ripe oocyte with SER (arrows), spherical mitochondria, lipid vesicles and transport vesicles. ×15,000. *Bar*: 500 nm.

O oocyte, *Ve* vitelline envelope, *G* granulosa cell, *Bm* basement membrane, *N* nucleus, *g* Golgi system, *RER* rough endoplasmic reticulum, *m* mitochondria, *l* lipid vesicle, *v* transport vesicle.

Figure 5-11

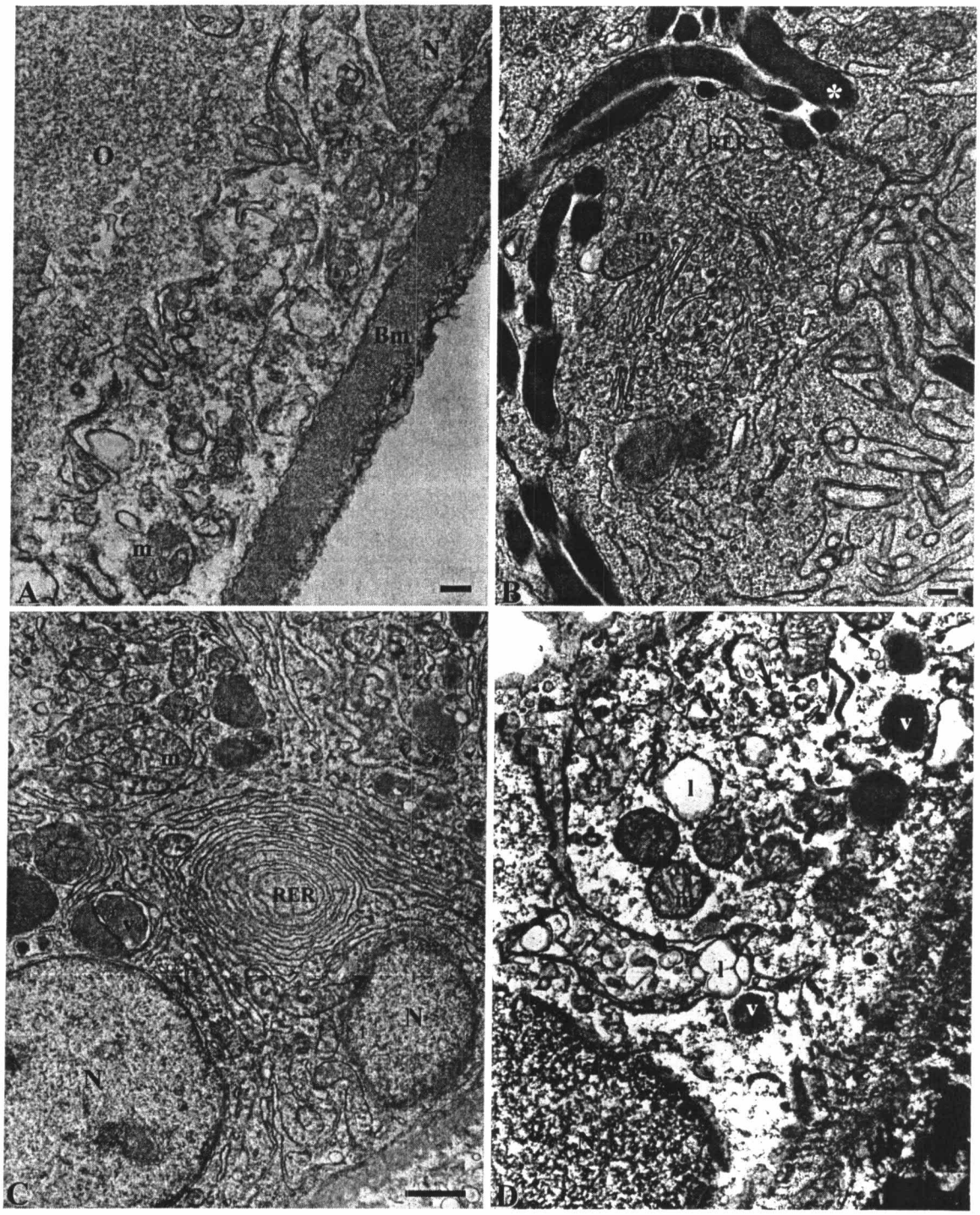

Figure 5-12: Electron micrograph of thecal cells of the control *O. niloticus*. (A) A thecal cell of perinucleolar oocyte with abundant globular SER (arrows). ×40,000. *Bar*: 200 nm. (B) A thecal cell of cortical alveolar oocyte. Mitochondria with tubulovesicular cristae (arrowhead), abundant globular SER (arrows) and transport vesicles are seen. ×20,000. *Bar*: 200 nm. (C) A thecal cell of vitellogenic oocyte with abundant mitochondria with electron-lucent inclusions, tubulovesicular cristae (arrowheads) and abundant globular SER (arrows). ×20,000. *Bar*: 200 nm. Inset: pleomorphic mitochondria with electron-dense and filamentous inclusions (double arrowheads). ×15,000. *Bar*: 500 nm.

N nucleus, *m* mitochondria, *pm* pleomorphic mitochondria, *v* transport vesicle.

Figure 5-12

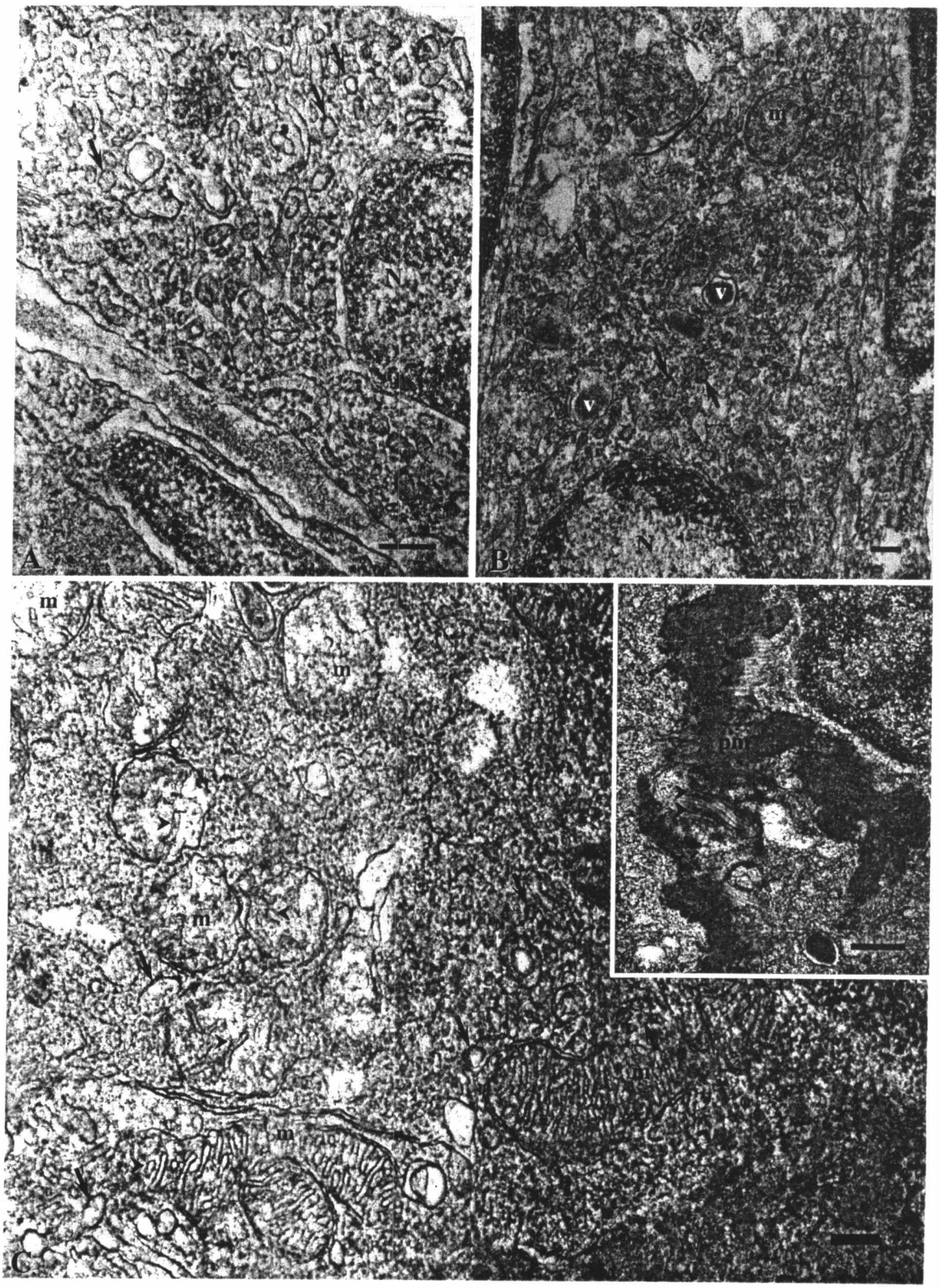

Figure 5-13: Electron micrograph of thecal cells of the treated *O. niloticus*. (A) A thecal cell of perinucleolar oocyte with abundant mitochondria with tubulovesicular cristae and globular SER (arrows). ×20,000. *Bar*: 200 nm. (B) A thecal cell of cortical alveolar oocyte shows myelin figures, large electron-dense vesicles and dilated ER. ×20,000. *Bar*: 200 nm. (C) A thecal cell of vitellogenic oocyte. Note the abundant elongated mitochondria with tubulovesicular cristae (arrowheads) and abundant globular SER (arrows). ×20,000. *Bar*: 200 nm.

N nucleus, *dER* dilated endoplasmic reticulum, *RER* rough endoplasmic reticulum, *m* mitochondria, *my* myelin figures, *v* transport vesicle.

Figure 5-13